# Phonon spectra and isothermal elastic constants for $f$-shell metals: A dynamical treatment

N. Singh and S. P. Singh
*Department of Physics, Maharshi Dayanand University, Rohtak 124 001, India*
(Received 13 February 1989; revised manuscript received 28 August 1989)

The two-body interaction is written as the sum of *s-s*,*d-d* overlap, *d-d* attractive, *f-f* overlap, and *f-f* attractive contributions. The free-electron part of the pair potential is obtained in second-order perturbation theory using a rational dielectric function and Heine-Abarenkov model pseudopotential. The overlap between *d* and *f* states of different ions and the effect of *s-d* and *s-f* hybridization are included in an approximate manner, as has been suggested by Wills and Harrison and by Harrison. The temperature dependence has been included through an asymptotic factor. The effective pair potential so defined is fast converging. It is then used to calculate the phonon spectra of rare-earth and actinide elemental metals in the fcc phase. The agreement between predicted and observed values is found to be reasonably good for all the metals. The binding energy and elastic constants of these metals are also calculated.

## I. INTRODUCTION

There exist several theories[1-5] in the literature that provide insight into the relative role played by the *s*- and *d*-like electrons in the screening of transition metals. An interesting result of these investigations is that many of the details of the band structure are quite inessential to the prediction of cohesive energy or bonding properties. Recently, Wills and Harrison[6] have obtained an effective pair potential by taking advantage of the separation between free-electron-like states exhibited in the transition-metal pseudopotential theory to treat the free-electron-like states with the simple-metal theory. The interaction among free electrons is treated by them in a Thomas-Fermi approximation. The overlapping contribution due to different *d* orbitals has been treated by combining one of the features of Andersen's muffin-tin orbital theory with the older transition-metal pseudopotential theory. A similar treatment of the *d*-state orthogonality matrix with a simple model of the *d*-band density of states is done. In rare-earth metals *f* bands play the role which the *d* bands play in transition metals. Therefore, Harrison,[7] in his subsequent paper, has treated *f* orbitals exactly in the same manner.

The Hartree dielectric function for the screening due to free electrons, with or without modifications, combined with the pseudopotential is being used to record the ion-ion interaction in the second-order perturbation theory.[8] The structure in the effective interaction is intimately associated with the logarithmic singularity at $q=2k_F$ in wave-number space. This logarithmic singularity does give rise to long-range Friedel oscillations, which in turn, are responsible for poor convergence for the ion-ion interaction. Most elemental metals do not have reciprocal lattice vectors spanning the Fermi surface and detecting the singularity. These very long-range oscillations must interfere destructively in the lattice sum. They will interfere constructively to help structural stability only in the vicinity of an average electron per atom ratio given by Mott and Zones[9] criterion of $Z$ equal to 1.36 for the fcc lattice and 1.48 for the bcc lattice. This suggests removing logarithmic singularity from the screening function for free electrons. The treatment of bonding properties of free electrons in *d*-band and *f*-shell metals in the Thomas-Fermi approximation is a sufficiently great simplification for calculating elastic and vibration properties. Nevertheless, it predicts the bulk properties almost for all the simple metals in the Periodic Table reasonably well.[10] The replacement of the Hartree dielectric function by the rational dielectric function[11] is a good choice for describing *s*-electron screening for the following reasons. (a) It reproduces the Lindhard function exactly and is free from the logarithmic singularity; (b) the calculations in wave-number space have indicated that the general form of the spectrum does not depend upon the singularity, while it does give a Kohn anomaly in the vibration spectrum; (c) the rational function has correct low- and high-$q$ behavior and is 0.5 at $q=2k_F$. The exchange-correlation corrections due to Taylor[12] have been included in the rational dielectric function through its parameters as these parameters are obtained by matching it with the Lindhard dielectric function modified for exchange-correlation corrections due to Taylor[12] by the least-squares fitting method; (d) the rational dielectric function combined with the pseudopotential theory gives rise to a simple analytic form of the ion-ion pair potential in second-order perturbation theory. The exponentially damped pair potential has the advantage of not containing the very long-range Friedel oscillations. This exponentially damped pair potential in combination with the ion-ion potential due to *d* electrons obtained by Wills and Harrison[6] is used by the authors[13] (hereafter it is referred as Paper I) to calculate elastic and vibrational properties of a number of transition metals. The purpose of the present paper is to extend the theory presented for transition metals in Paper I to *f*-shell metals. This is achieved by combining the exponentially damped pair potential with the contributions due to *d* and *f* electrons obtained by Wills and Harrison[6] and Harrison,[7] respectively.

 

## II. THE EFFECTIVE INTERACTION BETWEEN IONS

The total energy of a simple metallic system held at a fixed volume can be written as a sum of the volume-dependent terms and a term depending on the detailed arrangement of the ions as an effective two-body potential in the second-order pseudopotential perturbation theory as follows:[14]

$$E_{\rm BI}=E_{\rm EG}(n_0)+\tfrac{1}{2}V_{\rm BS}(r=0)+\tfrac{1}{2}\sum_{i(\neq 0)}V(\mathbf{r}_i)\ . \tag{1}$$

$E_{\rm EG}(n_0)$ is the energy of all the electrons in a homogeneous electron gas of density $n_0=NZ/V$, where $N$ and $Z$ are the number of atoms held in a volume $V$ and effective valence, respectively. The exchange-correlation corrections appropriate to the metallic densities[15] have been included in $E_{\rm EG}\ (n_0)$. $V_{\rm BS}\ (r=0)$ is obtained from the band-structure part of the energy by evaluating the integral appearing within it in conjunction with the rational dielectric function and the Heine-Abarenkov[16] model potential.

The derivation of $s$-$s$ interaction using the rational dielectric function is given in detail in Ref. 17. Here, we simply note that the part of the effective potential exactly cancels the electrostatic Coulomb repulsion and, within linear screening theory, the remainder is an effective screened Coulomb potential, given for a Heine-Abarenkov[16] model pseudopotential combined with the rational dielectric function by Eq. (2) of Ref. 18 (hereafter referred to as Paper II). We now consider the additional terms in the energy due to the coupling that broadens the $f$ states into bands. In calculating this contribution we may simply add the shift in eigenvalues of the occupied $f$ states. Harrison and Froyen[19] used their choice of the muffin-tin zero to write the denominator of a $f$-$f$ coupling matrix element taking a parabolic approximation for energy bands, and obtained the $f$-state coupling between ions separated along the quantization axis, which varies as the seventh power of the inverse internuclear spacing. Taking a simple rectangular model of density of $f$ states suggested by Friedel,[20] the first variation of the total energy from the bandwidth term can be expressed in terms of the potential[7]

$$V_f(r)=-Z_f\left[1-\frac{Z_f}{14}\right]\left[\frac{1}{n}\right]^{1/2}\frac{\hbar^2(5.06r_f)^5}{mr^7}\ , \tag{2}$$

if the ions were interacting with only nearest neighbors. $r_f$, $Z_f$, and $n$ are $f$-state radius, number of electrons in the $f$ band, and coordination number, respectively. $m$ is the mass of the electron in the $f$ band. The factor $Z_f[1-(Z_f/14)]$ represents the continuous filling of bonding through antibonding levels. Now, we need to include a term $V_{ff}(r)$ in the pair potential corresponding to the shift in $f$-band center. The fourth-order shift in the band center can be represented in terms of an overlap matrix element between perturbed states and $f$-$f$ matrix elements of different ion sites. Eventually, we get the nonorthogonal potential due to $f$ states as[7]

$$V_{ff}(r)=2Z_f\frac{\hbar^2(3.11r_f)^{10}}{mr^{12}}\ . \tag{3}$$

In the framework of the second-order perturbation theory, we write the temperature-dependent two-body interaction $V(r)$ between ions in the following form:

$$V(r)=[V_{\rm FE}(r)+V_{dd}(r)+V_d(r)+V_f(r)+V_{ff}(r)]\times\exp(-\pi k_B Tr/\hbar v_F)\ . \tag{4}$$

The contribution to the pair potential due to the overlap of $d$ states on different ions $V_{dd}(r)$ and due to the attractive $d$-bonding contribution $V_d(r)$ is the same as has been defined by Eqs. (30) and (32), respectively, of Ref. 6. The damping factor, $\exp(-\pi k_B Tr/\hbar v_F)$ has been obtained by Takanaka and Yamamoto[21] from the asymptotic expression for the temperature-dependent multi-ion interaction using one-electron Green function. Here, $v_F=\hbar k_F/m$ is the Fermi velocity and $k_B$ is the Boltzmann constant.

Using the interionic potential $V(r)$, we obtain the radial $K_r$ and tangential force constants given by

$$K_r=\frac{d^2V(r)}{dr^2}=K_r^{\rm FE}+K_r^{dd}+K_r^{d}+K_r^{ff}+K_r^{f}\ , \tag{5}$$

and

$$K_t=\frac{1}{r}\frac{dV(r)}{dr}\ ,=K_t^{\rm FE}+K_t^{dd}+K_t^{d}+K_t^{ff}+K_t^{f}\ , \tag{6}$$

where $K_r^{\rm FE}$ and $K_t^{\rm FE}$ are the same as have been defined by Eqs. (7) and (8), respectively, of Paper II. However, $K_r^{dd},K_r^{d},K_t^{dd},K_t^{d}$ are defined by Eqs. (12), (13), (15), and (16) of Ref. 13. The rest of the force constants arising due to $s$ and $f$ electron interactions can be evaluated very easily. The resulting expressions of these force constants are given below:

$$K_r^{f}=V_f(r)\left[\frac{56}{r^2}+\frac{14y}{r}+y^2\right]\exp(-yr)\ , \tag{7}$$

$$K_r^{ff}=V_{ff}(r)\left[\frac{156}{r^2}+\frac{24y}{r}+y^2\right]\exp(-yr)\ , \tag{8}$$

$$K_t^{f}=-V_f(r)\left[\frac{7}{r^2}+\frac{y}{r}\right]\exp(-yr)\ , \tag{9}$$

$$K_t^{ff}=-V_{ff}(r)\left[\frac{12}{r^2}+\frac{y}{r}\right]\exp(-yr)\ , \tag{10}$$

with

$$y=(\pi k_B T/\hbar v_F)\ .$$

From $K_r$ and $K_t$ at any interionic separation, we obtain the interionic force constant $K_{\alpha\beta}$, where both $\alpha$ and $\beta$ are Cartesian components $(x,y,z)$. From the interionic force constant $K_{\alpha\beta}$ at $n$th neighbor separation, we obtain the elastic moduli using the dynamical long-wavelength pho-

non method[22] and the dynamical matrix. For details we refer to Paper I.

## III. CALCULATIONS AND RESULTS

Lanthanum is a typical $d$-electron superconductor and recent band theoretical calculations[23] indicate that the $f$ bands lie approximately 2 to 2.5 eV above the Fermi level. The renormalization of the phonon spectrum is characterized by $d$ bands near the Fermi energy and it plays an important role in determining the phonon spectra of transition metals.[24] Therefore, the three valence electrons in La have been divided equally in $5d$ and $6s$ bands according to the prescription for transition metals due to Wills and Harrison.[6] The $f$ band in La is kept empty as has been suggested in Ref. 25. The electronic configurations $5d^{0.5}4f^{1}6s^{2.5}$, $5d^{0.5}4f^{14}6s^{1.5}$, and $6d^{0}5f^{1}7s^{3}$ are chosen for Ce, Yb, and Th, respectively, for the present calculations. We do not have $d$-band parameters for the rare earths as we did for the transition-metal series, but we expect that the successive addition of protons to the nucleus and electrons to the $f$ states concentrated near the nucleus would not change the $d$ states greatly. Therefore, we take the $d$-state radius equal to that of yttrium for all metals considered so far except for La. The $d$-state radius for La is taken equal to 1.286 a.u. The number of electrons in a $f$ band, $Z_f$, and $f$-state radius $r_f$ are taken to be the same as those given in Refs. 7 and 25. The electron density parameter $r_s$ is taken correspondingly to the observed volume.[26] The value of atomic radius for La at 660 K is extrapolated from the observed value of it with the help of the linear expansion coefficient data, which, in turn, is obtained from a Grüneisen constant and bulk modulus using Eq. (28) of Ref. 6. These are listed in Table I for convenience. The potential parameters are determined by matching the calculated phonon frequencies with the observed values for $[100]L$ and $[100]T$ modes in the long-wavelength region. This is equivalent to fit the elastic constants $C_{11}$ and $C_{44}$, respectively. The values of $D$ and $r_c$ so obtained are given in Table I. Our fitted value of $r_c$ for thorium is found larger than its value for cerium although $r_s(\mathrm{Ce}) > r_s(\mathrm{Th})$. This anomalous behavior of the core parameter $r_c$ is found in accordance with anomalous behavior shown by the observed phonon spectra of these metals. The measured values of phonon frequencies for Th are higher by about 13% than those for Ce although the atomic mass of thorium is larger than that of the Ce atom. Theoretical results of binding energy are presented in Table II and elastic constants calculated in the long-wavelength limit are given in Table III along with experimental[27–30] values. Meaningful, but not very accurate, results using the pair potential defined by Eq. (4) can be obtained including only a few nearest neighbors; here we carry each calculation to convergence. On the other hand, one has to include contributions beyond the tenth shell to get meaningful results using the two-body interaction defined with the Lindhard-Taylor[12] dielectric function; here we have included contributions up to the 32nd shell for La and Yb and up to the 48th shell for Ce and Th. The values of binding energy and elastic moduli obtained using the Lindhard-Taylor[12] dielectric function are also given in Tables II and III, respectively, for comparison. The elastic constants obtained using the two screening functions are almost the same as were expected. It is found that the radial force constants play a dominant role in yielding the elastic moduli. The radial force constant obtained using the pair potential defined with the Lindhard-Taylor[12] dielectric function is found to be slowly converging with interatomic separation for Ce and Th. One may get matching results by including the contributions beyond the 48th shell in these particular cases. It is to be noted that the calculated binding energy for Yb and Th is in better agreement with measured values of it than those for La and Ce. However, this anomaly can be removed by choosing more appropriate configurations, viz., $5d^{1}6s^{2}$ for La and $4f^{2}6s^{2}$ for Ce. For more details, see Table II.

The phonon frequencies of La, Ce, Yb, and Th along three principal symmetry directions are shown in Figs. 1–4 as obtained with Eqs. (4)–(10). It is found that the

TABLE I. Observed (Ref. 26) atomic radius $r_0$ and fitted values of the pseudopotential parameters $D$ and $r_c$ (a.u.). $(f)$, $(g)$, and $(h)$ represent the three configurations chosen for each elemental solid.

| | | $_{57}$La | | $_{58}$Ce |
|---|---|---|---|---|
| $r_0$ | | 3.961 | | 3.819 |
| $D$ | | 0.73 | | 0.80 |
| | | $r_c$ | | $r_c$ |
| $(f)$ | $5d^{1.5}6s^{1.5}$ | 2.80 | $5d^{0.5}4f^{1}6s^{2.5}$ | 2.43 |
| $(g)$ | $5d^{1}6s^{2}$ | 2.43 | $5d^{1}4f^{1}6s^{2}$ | 2.77 |
| $(h)$ | $5d^{0}6s^{3}$ | 2.21 | $5d^{0}4f^{2}6s^{2}$ | 2.55 |
| | | $_{70}$Yb | | $_{90}$Th |
| $r_0$ | | 3.762 | | 3.762 |
| $D$ | | 0.80 | | 0.89 |
| | | $r_c$ | | $r_c$ |
| $(f)$ | $5d^{0.5}4f^{14}6s^{1.5}$ | 2.73 | $6d^{0}5f^{1}7s^{3}$ | 2.58 |
| $(g)$ | $5d^{1}4f^{13}6s^{2}$ | 2.62 | $6d^{0.5}5f^{1}7s^{2.5}$ | 2.85 |
| $(h)$ | $5d^{0}4f^{14}6s^{2}$ | 2.17 | $6d^{1}5f^{0}7s^{3}$ | 2.53 |

TABLE II. Binding energy (eV/atom) obtained using Eq. (1) for La, Ce, Yb, and Th. Experimental values of binding energy are estimated using the empirical relation, $-E_{BI}=E_{coh}+E_Z$, from the data of cohesive energy and first, second, and third ionization energies $E_I$, $E_{II}$, and $E_{III}$, respectively, summarized in Refs. 35 and 36. $E_Z$ represents $E_I+\frac{1}{2}E_{av}$, $E_I+E_{II}$, $E_I+E_{II}+\frac{1}{2}E'_{av}$, and $E_I+E_{II}+E_{III}$, respectively, for $Z$ equal to 1.5, 2.0, 2.5, and 3.0, where $E_{av}=\frac{1}{2}(E_I+E_{II})$ and $E'_{av}=\frac{1}{2}(E_{II}+E_{III})$. ($f$), ($g$), and ($h$) represent the three configurations chosen for each elemental solid. The numbers written within parentheses represents the errors (%) present in calculated values.

| | | $_{57}$La | $_{58}$Ce | $_{70}$Yb | $_{90}$Th |
|---|---|---|---|---|---|
| Pettifor[a] | ($f$) | 11.711(−18) | 33.684(+19) | 13.303(+7) | 44.071(−1) |
| | ($g$) | 21.114(0) | 22.231(+8) | 23.044(+15) | 30.785(−5) |
| | ($h$) | 46.171(+15) | 21.406(+4) | 23.038(+15) | 45.820(+2) |
| Lindhard-Taylor[b] | ($f$) | 11.677 | 33.603 | 13.268 | 43.979 |
| | ($g$) | 21.090 | 22.148 | 22.986 | 30.730 |
| | ($h$) | 46.110 | 21.340 | 23.083 | 45.720 |
| Expt. | ($f$) | 14.206 | 28.403 | 12.455 | 44.600 |
| | ($g$) | 21.107 | 20.640 | 20.02 | 32.475 |
| | ($h$) | 40.282 | 20.640 | 20.02 | 44.600 |

[a]Results obtained using the Pettifor (Ref. 11) dielectric functions.
[b]Results obtained using the Lindhard-Taylor (Ref. 12) dielectric functions.

interionic potential reproduces the experimental[28–31] results of phonon spectra fairly well for all the metals except for the [111]$T$ mode of Ce where the discrepancies are quite large at a few wave vectors. The maximum discrepancy of 20% between the calculated and experimental results is found for the [111]$T$ mode at the zone boundary for all the three metals La, Yb, and Th. Recently, Onwuagba[32] and Wang and Overhauser[33] have calculated the phonon spectra of La and Yb, respectively, following altogether different approaches. Our calculated results are almost similar to their findings for both La and Yb. The results to demonstrate the relative magnitude of the phonon frequencies at the Brillouin-zone boundary arising due to $s$, $d$, and $f$ electrons are given in Table IV. It is found that both $d$ and $f$ electrons normalize the longitudinal modes considerably. The maximum contribution to the [111]$L$ mode of La, Ce, Yb, and Th due to $d$ or $f$ electrons or both, as the case may be, is found to be −5%, −30%, −17%, and −26%, respectively. The $d$ and $f$ electrons in Ce contribute equally ($\sim -15\%$) to phonon frequencies. The overlap contribution due to $f$ orbitals on different ions enhances the phonon modes at the most by 2% as the $f$ band in Yb is completely filled. The contributions up to the seventh shell have been found sufficient to achieve convergence. However, to achieve convergence of the same order in per-

TABLE III. Theoretical values of elastic constants are obtained at 300 K for Ce, Yb, and Th and at 660 K for La. Experimental results are taken from Refs. 27–30. ($a$) and ($b$) represent the results obtained using the Pettifor (Ref. 11) and the Lindhard-Taylor (Ref. 12) dielectric functions, respectively. ($f$), ($g$), and ($h$) represent the three configurations chosen for each elemental solid. The numbers written within parentheses represent the errors (%) in calculated values.

| | $C_{11}$ (Mbar) | | | $C_{12}$ (Mbar) | | | $C_{44}$ (Mbar) | | |
|---|---|---|---|---|---|---|---|---|---|
| | ($a$) | ($b$) | Expt. | ($a$) | ($b$) | Expt. | ($a$) | ($b$) | Expt. |
| $_{57}$La($f$) | 0.284(0) | 0.295 | 0.285 | 0.264(+29) | 0.277 | 0.204 | 0.153(−7) | 0.164 | 0.165 |
| ($g$) | 0.286(0) | 0.247 | | 0.182(−11) | 0.173 | | 0.151(−8) | 0.138 | |
| ($h$) | 0.296(+4) | 0.268 | | 0.118(−42) | 0.126 | | 0.120(−27) | 0.127 | |
| $_{58}$Ce($f$) | 0.244(+1) | 0.323 | 0.241 | 0.055(−46) | 0.052 | 0.102 | 0.183(−6) | 0.186 | 0.194 |
| ($g$) | 0.181(−25) | 0.085 | | 0.109(+7) | 0.088 | | 0.231(+19) | 0.206 | |
| ($h$) | 0.253(+5) | 0.198 | | 0.171(+67) | 0.158 | | 0.156(−20) | 0.141 | |
| $_{70}$Yb($f$) | 0.181(−3) | 0.192 | 0.186 | 0.148(+42) | 0.160 | 0.104 | 0.163(−8) | 0.175 | 0.177 |
| ($g$) | 0.172(−8) | 0.092 | | 0.066(−37) | 0.048 | | 0.232(+31) | 0.201 | |
| ($h$) | 0.223(+20) | 0.225 | | 0.115(+11) | 0.117 | | 0.098(−45) | 0.098 | |
| $_{90}$Th($f$) | 0.754(0) | 0.681 | 0.753 | 0.439(−10) | 0.430 | 0.489 | 0.385(−20) | 0.377 | 0.478 |
| ($g$) | 0.618(−18) | 0.763 | | 0.475(−3) | 0.470 | | 0.397(−17) | 0.400 | |
| ($h$) | 0.749(−1) | 0.678 | | 0.389(−21) | 0.384 | | 0.438(−8) | 0.432 | |

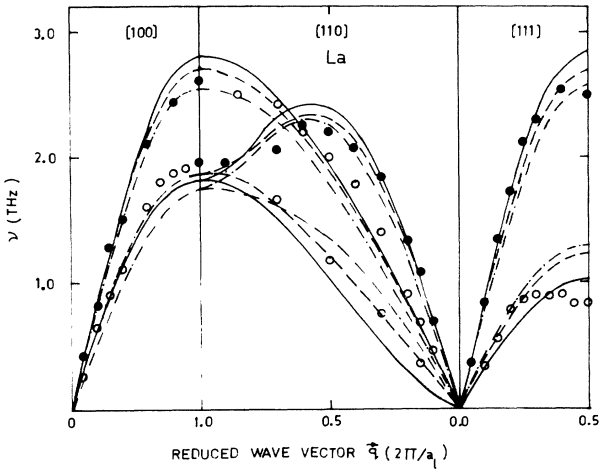


FIG. 1. Dispersion curves of La. The solid, dashed, and dot-dashed lines represent the present calculations at 660 K for the configurations $5d^{1.5}6s^{1.5}$, $6d^{1}6s^{2}$, and $5d^{0}6s^{3}$, respectively. The points are experimental data by Stassis *et al.* (Ref. 28) at 660 K. $a_l$ is the lattice parameter.

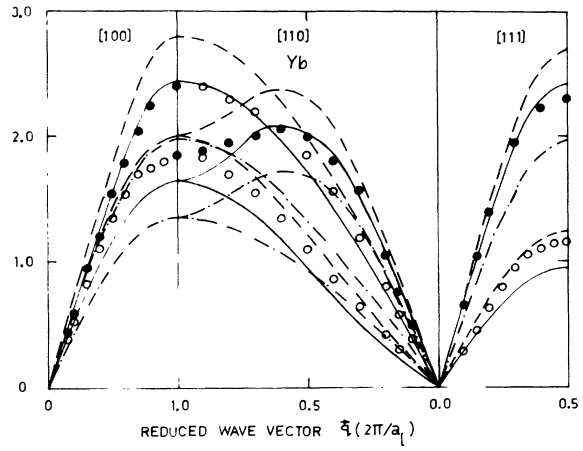


FIG. 3. Dispersion curves of Yb. The solid, dashed, and dot-dashed lines represent the present calculations at 300 K for the configurations $5d^{0.5}4f^{14}6s^{1.5}$, $5d^{1}4f^{13}6s^{2}$, and $4f^{14}6s^{2}$, respectively. The points are the experimental data by Stassis *et al.* (Ref. 30) at room temperature. $a_l$ is the lattice parameter.

forming the calculation of phonon spectra in the reciprocal space with usual practice, i.e., using the effective potential defined with the Lindhard function in the second-order perturbation theory, one has to include contributions up to the 16th shell. Thus, a numerical calculation of phonon spectra in all the seven branches of the three symmetry directions using the present pair potential requires about $\frac{1}{10}$ of the computer time compared to that required by the calculation of it in wave-number space at the same number of points using the Lindhard dielectric function. It is to be noted further that in the present method, there is no need of calculating the electrostatic Coulomb part of the phonon frequencies separately, as a part of the band-structure term exactly cancels the electrostatic Coulomb repulsion in the effective potential. For further details see Paper II.

In the pair potential defined by Eq. (4), *s-d* and *s-f* hybridization are included through the parameters $Z$, $Z_d$, and $Z_f$. Therefore, to see the effect of different choices of these parameters on the quantities calculated, we have repeated the calculations for the configurations $5d^{1}6s^{2}$, $5d^{0}6s^{3}$ for La; $5d^{1}4f^{1}6s^{2}$, $5d^{0}4f^{2}6s^{2}$ for Ce; $5d^{1}4f^{13}6s^{2}$, $5d^{0}4f^{14}6s^{2}$ for Yb and $6d^{0.5}5f^{1}7s^{2.5}$, $6s^{1}5f^{0}7s^{3}$ for Th. The parameters of the model potential for these

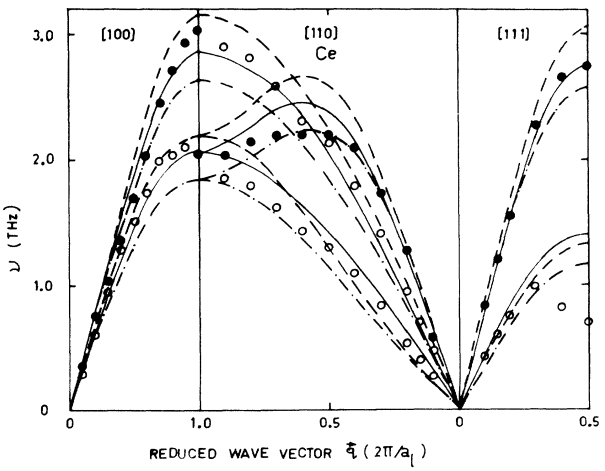


FIG. 2. Dispersion curves of Ce. The solid, dashed, and dot-dashed lines represent the present calculations at 300 K for the configurations $5d^{0.5}4f^{1}6s^{2.5}$, $5d^{1}4f^{1}6s^{2}$, and $4f^{2}6s^{2}$, respectively. The points are the experimental data by Stassis *et al.* (Ref. 29) at room temperature. $a_l$ is the lattice parameter.

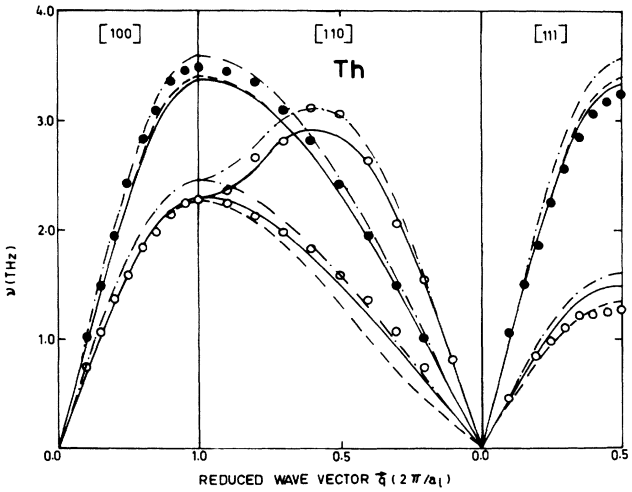


FIG. 4. Dispersion curves of Th. The solid, dashed, and dot-dashed lines represent the present calculations at 300 K for the configurations $6d^{0}5f^{1}7s^{3}$, $6d^{0.5}5f^{1}7s^{2.5}$, and $6d^{1}5f^{0}7s^{3}$, respectively. The points are the experimental data by Reese *et al.* (Ref. 31) at room temperature. $a_l$ is the lattice parameter.

TABLE IV. Longitudinal ($L$) and transverse ($T$) phonon frequencies at the Brillouin-zone boundary. $\nu\,(Z_d=0,Z_f=0)$, $\nu\,(Z_d=0)$, and $\nu\,(Z_f=0)$ represent the calculated results by putting off the contribution due to both $d$ and $f$, $d$, and $f$ electrons, respectively. $\nu$ represents the results obtained by including all possible contributions considered so far.

| | | $\nu\,(Z_d=0,Z_f=0)$ | $\nu\,(Z_d=0)$ | $\nu\,(Z_f=0)$ | $\nu$ | Expt. |
|---|---|---|---|---|---|---|
| La$\sim 5d^{1}\,^{5}6s^{1.5}$ | | | | | | |
| | [100]$L$ | | 2.96 | | 2.82 | 2.60 |
| | [100]$T$ | | 1.90 | | 1.83 | 1.95 |
| | [111]$L$ | | 3.00 | | 2.85 | 2.50 |
| | [111]$T$ | | 1.07 | | 1.03 | 0.84 |
| Ce$\sim 5d^{0}\,^{5}4f^{1}6s^{2.5}$ | | | | | | |
| | [100]$L$ | 3.58 | 3.23 | 3.24 | 2.85 | 3.04 |
| | [100]$T$ | 2.40 | 2.21 | 2.27 | 2.06 | 2.05 |
| | [111]$L$ | 3.60 | 3.22 | 3.19 | 2.76 | 2.75 |
| | [111]$T$ | 1.58 | 1.48 | 1.52 | 1.42 | 0.75 |
| Yb$\sim 5d^{0}\,^{5}4f^{14}6s^{1.5}$ | | | | | | |
| | [100]$L$ | 2.79 | 2.81 | 2.41 | 2.44 | 2.40 |
| | [100]$T$ | 1.78 | 1.80 | 1.62 | 1.64 | 1.85 |
| | [111]$L$ | 2.84 | 2.87 | 2.39 | 2.42 | 2.30 |
| | [111]$T$ | 1.01 | 1.03 | 0.94 | 0.96 | 1.16 |
| Th$\sim 5f^{1}7s^{3}$ | | | | | | |
| | [100]$L$ | | | 4.15 | 3.36 | 3.47 |
| | [100]$T$ | | | 2.71 | 2.30 | 2.26 |
| | [111]$L$ | | | 4.21 | 3.34 | 3.24 |
| | [111]$T$ | | | 1.73 | 1.51 | 1.28 |

configurations have been adjusted again as have been described earlier and are given in Table I. The calculated values of the binding energy and the elastic constants using new parameters are shown in Tables II and III, respectively. The results of phonon spectra calculated for the present configurations are also shown in Figs. 1–4. It is found that the longitudinal phonon modes near the Brillouin-zone boundary soften most as we increase the number $Z$ or decrease $Z_d$ or $Z_f$. This is equivalent to increasing the ionic screening due to $s$ electrons, which tends to soften the phonon modes near the zone boundary. It is found that the configurations $5d^{1}6s^{2}$, $5d^{0.5}4f^{1}6s^{2.5}$, $5d^{0.5}4f^{14}6s^{1.5}$, and $5f^{1}7s^{3}$ yield overall better results for all the three properties, viz., the binding energy, the elastic constants, and the phonon spectra for La, Ce, Yb, and Th, respectively.

## IV. CONCLUSIONS

In summary, we have utilized a number of approximations to obtain the theoretical expression for the pair potential of rare earths and actinides.[34] These approximations include use of the Friedel model of the density of states, low-order perturbation theory in the $f$ state conduction-band coupling, use of rational dielectric function, and the Heine-Abarenkov[16] model pseudopotential in treating the conduction electrons. Use of the rational dielectric function has eliminated the complexity and slow convergence of the two-body interaction for $s$ electrons obtained using the Hartree dielectric function. The calculated elastic and dynamical properties are in good accord with observed values in the light of the enormous simplifications allowed by the theory. This effective potential is the generalization of a transition-metal effective potential to $f$-band metals. The use of this pair potential for calculating the elastic and dynamical properties of a metal reduces the computer time manifold.

## ACKNOWLEDGMENTS

We wish to thank Professor D. G. Pettifor for helping us in calculating the parameters of the rational dielectric function. The authors are also grateful to Professor K. N. Pathak, Professor S. Prakash, and Professor H. H. Lal for their help. This work is supported by the University Grants Commission, New Delhi. The computer facility provided at the Computer Center, Maharshi Dayanand University, Rohtak, is gratefully acknowledged.

[1]V. L. Morruzi, A. R. Williams, and J. F. Janak, Phys. Rev. B **15**, 2854 (1977).
[2]O. K. Andersen, Phys. Rev. B **12**, 3060 (1975).
[3]A. R. Makintosh and O. K. Andersen, in *Electrons at the Fermi Surface*, edited by M. Springford (Cambridge University Press, Cambridge, 1979).
[4]D. G. Pettifor, J. Phys. F **7**, 613 (1977).
[5]D. G. Pettifor, J. Phys. F **7**, 219 (1978).

[6]J. M. Wills and W. A. Harrison, Phys. Rev. B **28**, 4363 (1983).
[7]W. A. Harrison, Phys. Rev. B **28**, 550 (1983).
[8]W. A. Harrison, *Pseudopotentials in the Theory of Metals* (Benjamin and Cummings, California, 1966).
[9]N. F. Mott and H. Jones, *Properties of Metals and Alloys* (Dover, New York, 1936), Chap. 7.
[10]J. M. Wills and W. A. Harrison, Phys. Rev. B **25**, 5007 (1982).
[11]D. G. Pettifor, Phys. Scr. **T1**, 26 (1982).
[12]R. Taylor, J. Phys. F **10**, 1699 (1978).
[13]N. Singh, N. S. Banger, and S. P. Singh, Phys. Rev. B **38**, 7415 (1988).
[14]M. W. Finnis, J. Phys. F **4**, 1645 (1974).
[15]D. Pines, *Elementary Excitations in Solids* (Benjamin, Amsterdam, 1963).
[16]V. Heine and D. L. Weaire, in *Solid State Physics,* edited by H. Ehrenreich, F. Seitz, and D. Turnbull (Academic, New York, 1970), Vol. 24.
[17]D. G. Pettifor and M. A. Ward, Solid State Commun. **49**, 291 (1984); M. A. Ward, Ph.D. thesis, Imperial College, London, England, 1985.
[18]N. Singh, N. S. Banger, and S. P. Singh, Phys. Rev. B **39**, 3097 (1989).
[19]W. A. Harrison and S. Froyen, Phys. Rev. B **21**, 3214 (1980).
[20]J. Friedel, in *The Physics of Metals,* edited by J. M. Ziman (Cambridge University Press, New York, 1969).
[21]K. Takanaka and R. Yamamoto, Phys. Status Solidi B **84**, 813 (1977).
[22]G. L. Squires, Ark. Fys. (Sweden) **25**, 21 (1963).
[23]W. E. Pickett, A. J. Freeman, and D. D. Koelling, Phys. Rev. B **22**, 2695 (1980).
[24]C. M. Verma and W. Weber, Phys. Rev. Lett. **39**, 1094 (1977); Phys. Rev. B **19**, 6142 (1979).
[25]W. A. Harrison, Phys. Rev. B **29**, 2917 (1984).
[26]W. B. Pearson, *A Handbook of Lattice Spacings and Structure of Metals and Alloys* (Pergamon, New York, 1958).
[27]H. B. Huntington, in *Solid State Physics,* edited by F. Seitz and D. Turnbull (Academic, New York, 1958), Vol. 7.
[28]C. Stassis, C. K. Loong, and J. Zarestky, Phys. Rev. B **26**, 5426 (1982).
[29]C. Stassis, T. Gould, O. D. McMasters, and K. A. Gschneider, Jr., and R. M. Nicklow, Phys. Rev. B **19**, 5746 (1979).
[30]C. Stassis, C. K. Loong, C. Theisen, and R. M. Nicklow, Phys. Rev. B **26**, 4106 (1982).
[31]R. A. Reese, S. K. Sinha, and D. T. Peterson, Phys. Rev. B **8**, 1332 (1973).
[32]B. N. Onwuagba, Phys. Status Solidi B **146**, 131 (1988).
[33]Y. R. Wang and A. W. Overhauser, Phys. Rev. B **35**, 501 (1987).
[34]J. M. Wills and W. A. Harrison, Phys. Rev. B **29**, 5486 (1984).
[35]C. Kittel, *Introduction to Solid State Physics,* 5th ed. (Wiley, New York, 1976).
[36]*CRC Handbook of Chemistry and Physics,* edited by R. C. Weast and M. J. Astle, 61st ed. (Chemical Rubber Company, Florida, 1980).